Deuteron NMR resolved mesogen vs. crosslinker molecular order and reorientational exchange in liquid single crystal elastomers

Journal:	*Physical Chemistry Chemical Physics*
Manuscript ID	CP-ART-10-2015-006207.R2
Article Type:	Paper
Date Submitted by the Author:	06-Jan-2016
Complete List of Authors:	Milavec, Jerneja; Jozef Stefan Institute; Jožef Stefan International Postgraduate School Domenici, Valentina; University of Pisa, Dipartimento di Chimica e Chimica Industriale Zupancic, Blaz; Jozef Stefan Institute, Resetic, Andraz; Jozef Stefan Institute; Jožef Stefan International Postgraduate School Bubnov, Alexej; Academy of Sciences of the Czech Republic, Institute of Physics Zalar, Bostjan; Jozef Stefan Institute; Jožef Stefan International Postgraduate School

Journal Name

ARTICLE

Deuteron NMR resolved mesogen vs. crosslinker molecular order and reorientational exchange in liquid single crystal elastomers

Received 00th January 20xx,
Accepted 00th January 20xx

DOI: 10.1039/x0xx00000x

www.rsc.org/

J. Milavec[a,b], V. Domenici[c], B. Zupančič[a], A. Rešetič[a,b], A. Bubnov[d], B. Zalar[a,b]

Differences in the temperature behaviour of orientational ordering of structurally equivalent side-chain liquid single crystal elastomers (LSCEs), ^{2}H-labelled in the crosslinker and mesogen, have been studied by deuteron quadrupole-perturbed NMR. The impact of nematic director reorientations on the deuteron NMR spectral shapes was analyzed in terms of discrete reorientational exchange model. This provided for the determination of the degree of nematic director alignment and for the quantification of the influence of the reorientational exchange on the ^{2}H NMR spectra in terms of two parameters, the nematic director orientational dispersion parameter σ_θ and the motional effectiveness parameter α. Comparative analysis of model simulations and experimental spectra reveals that mesogenic molecules in LSCEs exhibit faster reorientational dynamics as compared to crosslinker molecules and that mesogens and crosslinkers exhibit similar and rather substantial static director orientational disorder.

Introduction

Liquid crystal elastomers (LCEs) are materials in which orientational order of conventional liquid crystals is combined with the elasticity of polymer networks[1–3]. Many interesting properties are expected to emanate from the coupling between the nematic liquid crystalline order and elastic deformation, among them the giant thermomechanical response[4]. One of the most exciting features of these materials is their macroscopic form change, originating from the order-disorder transition of mesogens. Unidirectional alignment of domains in the sample is usually achieved by mechanical stretching during the preparation,[5] leading to the so called liquid single crystal elastomers (LSCEs). LSCEs are shape-memory materials, due to the ability to memorize the macroscopic shape under specific conditions[6]. With increasing temperature, monodomain LSCEs typically exhibit spontaneous mechanical contraction, related to disordering of mesogenic molecules, attached to the polymer backbone[1,7]. These materials are promising candidates for different technological applications, such as artificial muscles, smart surfaces, microelectromechanical systems (MEMS), and nanoelectromechanical systems (NEMS)[8–11].

LSCEs are multicomponent systems, consisting of a polymer backbone and one or several different types of crosslinking moieties and mesogens. In general, individual components may exhibit different degrees of orientational ordering and segmental dynamics. In previous studies[4,12,13], this aspect of LSCE systems has never been addressed in a greater detail. Specifically, no comparative studies targeted towards elucidating possible differences in the static orientational ordering and reorientational dynamics of crosslinker vs. mesogen have been performed so far. ^{2}H NMR has proved to be very useful in the investigations of paranematic-nematic phase transformation behavior of these interesting materials[4,12–15]. For this reason, we decided to employ this spectroscopic method on a series of conventional and newly synthesized siloxane-based side-chain LSCEs, providing for component-resolved, i.e. crosslinker vs. mesogen, sensitivity.

Our methodology is based on the conjecture that individual reorientational dynamics of resolved elastomer network components impacts their respective NMR spectra. In a LSCE network, typical molecular motions are: (i) high-frequency reorientations of the molecule about its long axis and rotational diffusion of the long molecular axis, determining the local nematic order parameter S and its director $\mathbf{n}$; (ii) collective fluctuations of the nematic field, with an intermediate timescale, and (iii) reorientations $\mathbf{n}$ mediated by local translational displacements (RMTD mechanism[16]), with a rather long timescale set by molecular translational diffusion in an environment with spatially inhomogeneous nematic director field[17,18].

The impact of individual dynamic processes on the motional narrowing of NMR spectra is determined by the exchange effectiveness parameter

$$\alpha = (\Delta\omega_{\mathrm{r.l.}}\tau_{\mathrm{exch}})^{-1} = (2\pi)^{-1}\,\nu_{\mathrm{exch}}/\Delta\nu_{\mathrm{r.l.}}\,, \qquad (1)$$

---

[a] Department of Condensed Matter Physics, J. Stefan Institute, Jamova 39, SI-1000 Ljubljana, Slovenia
[b] Jožef Stefan International Postgraduate School, SI-1000 Ljubljana, Slovenia
[c] Dipartimento di Chimica e Chimica Industriale, Universitá degli studi di Pisa, via Moruzzi 3, 56124 Pisa, Italy
[d] Institute of Physics, Academy of Sciences of the Czech Republic, Na Slovance 2, 182 21 Prague 8, Czech Republic

i.e. by the ratio between the exchange frequency $\nu_{\rm exch} = \tau_{\rm exch}^{-1}$ and the “rigid lattice” spectral line width $\Delta\nu_{\rm r.l.} = \Delta\omega_{\rm r.l.}/2\pi$. Here $\tau_{\rm exch}$ quantifies the characteristic timescale of the exchange process among instantaneous (rigid lattice) molecular states. In the “fast motion” regime, when the motion’s characteristic correlation time $\tau_{\rm exch}$ is relatively short, equivalently $\alpha \gg 1$, motional narrowing sets in and the inhomogeneous spectrum is completely averaged-out into a homogeneously broadened Lorentzian spectral line with respective homogeneous line width $fwhm_{\rm exch}$, resulting in an increased homogeneous linewidth[17]

$$fwhm_{\rm hom} = (\pi T_2)^{-1} = \left(\pi\widetilde{T}_2\right)^{-1} + fwhm_{\rm exch}. \qquad (2)$$

T_2 is the spin-spin relaxation time, determinable using conventional solid-echo pulse techniques, whereas $\widetilde{T}_2$ describes the contribution to transverse relaxation of nuclear magnetization from processes not associated with motional narrowing. Fast motion regime is encountered in liquid crystals at high temperatures, in the isotropic state, where a single line reflecting the absence of orientational order ($S = 0$) is found at the Larmor frequency, with the total line width $fwhm$ matching $fwhm_{hom}$. With decreasing temperature, reorientational motions are slowed-down, $\tau_{\rm exch}$ increases and, consequently, T_2 becomes shorter, resulting in increasing $fwhm_{\rm hom}$ with decreasing temperature. For even slower molecular motions, with the characteristic correlation time in the range where $\alpha \approx 1$, motional narrowing becomes incomplete, the spectral lines become non-Lorentzian, and the transversal relaxation becomes non-exponential. Moreover, in this regime the line shape is extremely sensitive to changes in α and consequently to changes in $\tau_{\rm exch}$. The $fwhm$ and $fwhm_{\rm hom}$ do not match anymore since in this “intermediate motion” regime spectral lines are only partially averaged out. In the “slow motion” regime ($\alpha \ll 1$), the molecular motions are too slow to affect the NMR line shape and there are no motional averaging effects. This is why at low temperatures, e.g. in the crystal phase of a liquid crystal elastomer, the spectrum is inhomogeneously broadened and reflects the distribution of instantaneous molecular orientational and conformational states, i.e. the “rigid lattice” state of the system[18,19]. Specifically, if this distribution is isotropic, a Pake-pattern spectral shape is obtained in the rigid lattice limit[20].

In the specific case of deuteron-labelled molecules (either mesogen or crosslinker), the impact of molecular reorientational dynamics is best estimated by considering the shift of the ^{2}H quadrupole-perturbed NMR absorption line doublet (± sign) as a function of parameters S, β, and θ:

$$\nu^{\pm} = \pm\tfrac{3}{4}\nu_q S P_2(cos\beta) P_2(cos\theta) = \pm\tfrac{3}{4}\bar{\nu}_q S P_2(cos\theta). \qquad (3)$$

Here ν_q is the quadrupole frequency of the deuteron in a C-D bond, typically 180 kHz[21], and P_2 are the second Legendre polynomials of the angle θ between the nematic director $\mathbf{n}$ and the external magnetic field and of the angle β between the C-D bond and the molecular long axis, respectively. Specifically, $\beta \approx 60°$ for the planar hexagonal geometry of the C-D bond in the case of phenyl ring deuteration. The respective effective quadrupole frequency is $\bar{\nu}_q \approx 22\ \mathrm{kHz}$. S is the nematic order parameter. Both $\bar{\nu}_q$ and S are averages, the former over reorientations of C-D bond about the long molecular axis (for the case of phenyl ring deuteration) and the latter over reorientational fluctuations of the long molecular axis. The inverse characteristic times of these two processes are much shorter than the width of inhomogeneous frequency distribution $\Delta\nu_{\rm r.l.} \approx 3/4 \cdot \nu_q \approx 3/4 \cdot 180$ kHz scanned by the reorienting and conforming molecule in the course of time. It is thus plausible to assume that, with respect to both processes, ^{2}H quadrupole-perturbed NMR probes the system in the complete motional narrowing limit. Nevertheless, below the nematic-isotropic transition temperature, although still fast enough for complete motional narrowing, molecular reorientations are biased (non-isotropic), a situation described by $S \neq 0$ that leads to onset of doublet splitting (Eq. (3)).

Dynamical processes may also exist in LSCEs, which modulate S and $P_2(cos\theta)$ on much longer timescales, e.g. processes resembling the RMTD mechanism. In a network with statically misaligned domains and no inter-domain mesogen exchange (“rigid lattice” regime in view of reorientations of director $\mathbf{n}$) the spectrum exhibits inhomogeneous broadening, reflecting the distribution of directors through the $P_2(cos\theta)$ term of Eq. (3). However, in the case when either (i) the mesogen molecule performs translational diffusion across domains with misaligned directors, or (ii) the domain director fluctuates in time, motional averaging of the spectrum is to be anticipated. We will demonstrate that it is indeed the case with ^{2}H quadrupole-perturbed NMR of selectively labelled side-chain LSCEs. Specifically, by considering nematic domain misalignment, equivalently a static distribution of director orientations θ, we show that the respective rigid lattice line width $\Delta\nu_{\rm r.l.}$ and the characteristic frequency of the reorientational exchange $\nu_{\rm exch}$ satisfy $\alpha \approx 1$ (Eq. (1)). One thus deals with intermediate motional narrowing regime where the spectral shapes reflect even minor differences in the timescale $\tau_{\rm exch}$ of reorientational dynamics of mesogen vs. crosslinker.

Experimental

Materials and methods

^{2}H quadrupole-perturbed NMR spectroscopy. ^{2}H NMR experiments were carried out with a Bruker Advance III 500 MHz high-resolution solid-state NMR spectrometer, equipped with an 11.74 T Bruker Ultrashield superconducting magnet, at the Larmor frequency of 76.753 MHz for deuterons. Spectra were recorded as a function of temperature by applying the solid-echo sequence ($90°_x$ - τ - $90°_y$ - τ - acquisition) with a 90° pulse of 3.8 μs and “exorcycle”[22] phase cycling. The echo delay τ was fixed to 10 μs and the delay between consecutive acquisitions was 28 ms. Measurements were performed on a strip-like, 0.2 mm thick sample of about 4 mm × 8.5 mm area. In our geometry, the long edge of the sample, the nematic director (oriented along the long edge), and spectrometer field were all pointing vertically. Temperature was controlled to within 0.1 K accuracy. Thermal equilibration of the sample took about 1000 s at each temperature. Lorentzian line fitting was employed to quantitatively determine the line widths of the spectral lines.

Transverse relaxation time T_2 was measured by varying τ in the solid-echo sequence, in the temperature range between 370 K and 300 K. The variable time delay τ ranged from 10 μs to 20 ms (10 values) and 1024 - 20480 scans have been acquired for each spectrum. T_2 values were determined by fitting the experimental integrals of the quadrupole-perturbed ^{2}H spectra as a function of τ by using exponential decay function.

Preparation of Liquid Single Crystal Elastomers. Several monodomain LSCE samples were made by thermal polymerization followed by the two step crosslinking "Finkelmann procedure"[5]. A pre-polymerization mixture was prepared by adding the poly(methylhydrosilane), the crosslinker V1 (15% mmol units), the nematogen M4 (33.6% mmol units) and the smectogen M11 (51.5% mmol units) (see Scheme 1) to a 2.2 ml of anhydrous toluene. 30 μl of commercial platinum catalyst (COD from Wacker Chemie) was added to the final mixture. In a single sample, only one of the components was used in a deuterated version, which allowed for selective ^{2}H NMR measurements. Preparation of V1, M4, M11 and their deuterated homologues is reported elsewhere[23,24]. The prepared mixture was inserted in a circular reactor inside a temperature-controllable centrifuge. A rate of 5500 rpm (revolutions per minute) and a temperature of 343 K were set for 1 h in order to obtain, in the first step, a partially crosslinked elastomeric network in the form of a film (dimensions 15 mm × 215 mm and thickness of about 0.3 mm). After the spinning, partially crosslinked film was removed from the form and then loaded mechanically in a gradual manner by adding weights at room temperature. Finally, the sample was dried for 3 days at 343 K and at constant mechanical load.

Scheme 1. Chemical constituents of the LSCE film: (a) nematogen M4, (b) smectogen M11, and (c) crosslinker V1. X denotes ^{2}H in selectively labelled compounds.

Results and discussion

Director reorientation mechanism and domain misalignment

To estimate which motion regime should be assigned to our spectra of monodomain LSCE ^{2}H-labelled on mesogen or crosslinker molecules, the homogeneous line width and total line width of spectral lines are compared (Fig. 1). In LSCEs with ^{2}H-labelled mesogen, the matching between the homogeneous line width $fwhm_{\text{hom}}$ in the nematic phase and the total line width of the spectral line is better when compared to ^{2}H crosslinker-labelled LSCEs. This suggests that, assuming imperfect domain alignment, director reorientations result in a stronger motional narrowing in the case of mesogen molecules than in the case of crosslinker molecules, suggesting a scenario of less restricted reorientational dynamics for the case of mesogen.

In the paranematic phase[25], one can observe an almost complete matching between homogeneous and total line width for ^{2}H mesogen-labelled LSCEs. Higher temperature results in a faster translation diffusion and therefore the averaging is more effective, while the variations of order parameter are small.

Figure 1. Comparison of homogenous line width (as calculated from T_2 measurements) and total linewidth for LSCEs ^{2}H labelled on (a) mesogen and (b) crosslinker.

In the following, we will analyze the impact of the director reorientation process on the shape of ^{2}H NMR spectra in the framework of a discrete reorientational exchange model, in order to obtain more detailed information on the degree of domain alignment, particularly in view of its temperature dependence. We shall demonstrate that domain misalignment and RMTD-like director reorientations in LSCEs can well be quantified by only two parameters, the domain order parameter Q_{stat} and the characteristic orientational order decay time τ_Q.

Theoretical Calculations

To account for non-ideal director alignment in oriented LSCEs, we model the static (equilibrium) distribution of orientations of domain director $w_{\text{stat}}(u,\sigma_\theta)$ as a "spherical" Gaussian,

$$w_{\text{stat}}(u,\sigma_\theta) = \frac{e^{-\frac{1-u^2}{2\tan^2\sigma_\theta}}}{e^{-\frac{1}{2\tan^2\sigma_\theta}}\sqrt{2\pi}\,\tan\sigma_\theta \operatorname{erfi}\left(\frac{1}{\sqrt{2}\tan\sigma_\theta}\right)}. \qquad (4)$$

Here $u = \cos\theta \in [-1,1]$, with θ denoting the local orientation of a nematic domain. Misalignment of nematic domains is quantified by the angular dispersion parameter σ_θ. Specifically, $\sigma_\theta = 0°$ corresponds to $w_{\text{stat}}(u) = [\delta(u-1)+\delta(u+1)]/2$, i.e., to ideal LSCE sample with perfectly aligned domains, whereas $\sigma_\theta = 90°$ models a polydomain sample with isotropic domain distribution $w_{\text{stat}}(u) = 1/2$. Erfi is the imaginary error function.

We find the reorientational exchange among states parametrized by u to be most efficiently modelled by employing the algebra developed to describe the impact of chemical exchange processes on the NMR line shape[17,26]. Specifically, we discretize the $[-1,1]$ interval of continuous variable u into N discrete intervals Δu_k with respective rigid lattice frequencies $\langle\nu\rangle_k^{\pm}$ and allow jumps among sites indexed by $k = 1,\cdots,N$. $\langle\cdots\rangle$ denotes averages of $\nu^{\pm}(u)$ (Eq. (3)) over w_{stat} within Δu_k. The latter are chosen so that static probabilities $P_{\text{stat},k}$, corresponding to integrals of probability density w_{stat} over u across Δu_k, do not depend on k, i.e., $P_{\text{stat},k} = 1/N$. A detailed description of this procedure is given in the Electronic Supplementary Information. The resulting ^{2}H quadrupole-perturbed spectrum can be expressed as[18]

$$\mathcal{J}(\nu;\bar{\nu}_q,S,\sigma_\theta,\alpha) \propto \mathcal{J}^{+}(\nu;\bar{\nu}_q,S,\sigma_\theta,\alpha) + \mathcal{J}^{-}(\nu;\bar{\nu}_q,S,\sigma_\theta,\alpha)$$

(5a)

where

$$\mathcal{J}^{\pm}(\nu;\bar{\nu}_q,S,\sigma_\theta,\alpha)=$$

$$=\mathrm{Re}\left\{\boldsymbol{P}_{\mathrm{stat}}^{\mathsf{T}}\left[i2\pi\left(\underline{\mathbf{v}}^{\pm}(\bar{\nu}_q,S,\sigma_\theta)-\nu\underline{\mathbf{I}}\right)-\right.\right.$$

$$\left.\left.-\widetilde{T}_2^{-1}\,\underline{\mathbf{I}}+2\pi\Delta\nu_{\mathrm{r.l.}}(\bar{\nu}_q,S,\sigma_\theta)\alpha\tilde{\tau}_Q(\sigma_\theta)\underline{\mathbf{K}}\right]^{-1}\boldsymbol{P}_{\mathrm{stat}}\right\}$$

(5b)

$\underline{\mathbf{v}}^{\pm}(\bar{\nu}_q,S,\sigma_\theta)$ is the diagonal matrix of frequencies $\nu_k^{\pm}$, $\underline{\mathbf{I}}$ the identity matrix, whereas $\widetilde{T}_2$ describes the inherent spin-spin relaxation time (Eq. (2)). $\underline{\mathbf{K}}$ is the dimensionless population exchange matrix, with the pre-factor product of rigid-lattice line width $\Delta\nu_{\mathrm{r.l.}}(\bar{\nu}_q,S,\sigma_\theta)$, exchange effectiveness α, and dimensionless characteristic time $\tilde{\tau}_Q(\sigma_\theta)$ of the orientational order decay, independent of the exchange timescale. $\boldsymbol{P}_{stat}=(1,1,\cdots,1,1)/N$ is the vector of stationary probabilities of states k. Using the above approach, the calculation of NMR spectra is reduced to finding the inverse of a $N\times N$ matrix (see relation (5b)). Within this scenario, the exchange timescale τ_{exch} is set by the orientational correlation time τ_Q, given implicitly via $\alpha=\left(2\pi\Delta\nu_{\mathrm{r.l.}}\tau_Q\right)^{-1}$.

Comparison of simulated and experimental deuteron NMR spectra

Network component-resolved orientational order of structurally equivalent LSCEs was determined by studying temperature dependences of ^{2}H NMR spectra across the paranematic–nematic phase transition of samples, ^{2}H-labelled on either mesogen or crosslinker molecule (Fig. 2). LSCEs are inherently multicomponent systems, so that differences in orientational self-organization necessarily occur even between the mesogen and the crosslinker. This is apparently the case in our LSCE networks: at the transition from the high-temperature paranematic phase into low-temperature nematic phase, the crosslinker exhibits a significantly stronger orientational disorder than the mesogen. We relate this observation to the fact that molecules of crosslinker are connected by both ends to the polymer chain. Consequently, they are geometrically more confined and exhibit slower overall reorientational dynamics as compared to the mesogen molecules, attached to the backbone at one end only. The consequence of comparatively slower crosslinker dynamics and, consecutively, less effective motional averaging of the spectral lines, are broader spectral features and lower spectral resolution as compared to mesogen molecules. Faster director reorientational dynamics therefore leads to a stronger motional narrowing of mesogen spectral lines compared to crosslinker spectral lines. This renders the spectra of mesogen apparently less inhomogeneously broadened. Within this refined scenario, mesogens and crosslinkers exhibit very similar degree of a rather substantial director orientational disorder, and the observed differences in the ^{2}H NMR spectra are due to motional narrowing.

In order to resolve the above ambiguity, a selection of simulated spectra, calculated with discrete reorientational exchange model and the corresponding experimentally determined spectra of monodomain LCEs are compared in Fig. 2. Simulated spectra were generated with $\bar{\nu}_q=22$ kHz and experimental $T_2'\gtrsim(\pi fwhm_{\mathrm{hom}})^{-1}$ values (Fig. 1 and Eq. (2)) by adjusting the three fitting parameters S, σ_θ, and α at each temperature to best fit the experimental spectra. The number of exchange sites was set to $N=100$ in the weak-collision limit ($\Delta N=3\ll N$) in order to obtain sufficiently high resolution. $\tilde{\tau}_Q(\sigma_\theta)$ was calculated using the approach described in the Supplemental and $\Delta\nu_{\mathrm{r.l.}}(\bar{\nu}_q,S,\sigma_\theta)$ was approximated with $\Delta\nu_{\mathrm{r.l.}}\approx\bar{\nu}_q S$.

Figure 2: ^{2}H NMR spectra, recorded from the paranematic to the nematic phase (panel (a) for LSCE labelled on the M4 mesogen and panel (c) for LSCE labelled on the V1 crosslinker) and calculated using the reorientational exchange model of the nematic director (panel (b) for the mesogen and panel (d) for the crosslinker, respectively).

While fitting, we allowed for discrepancies in σ_θ and α between the mesogen- and crosslinker-labelled specimen, whereas we imposed identical $S(T)$ profile. The criterion of acceptable fits was matching of doublet splitting $\Delta\nu_q$ to within 5% and matching of truncated second moment $M_2=\int_{-\nu_{\mathrm{tr}}}^{+\nu_{\mathrm{tr}}}\nu^2\mathcal{J}(\nu)d\nu$ to within 20% with truncation frequency $\nu_{\mathrm{tr}}=20$ kHz. The resulting $\Delta\nu_q(T)$ and $M_2(T)$, shown in Fig. 3, reveal satisfactory optimization of theoretical predictions to experimental values in the whole temperature range for both labelling sites.

Figure 3. Comparison of experimental (solid circles) and theoretical (open circles) temperature dependences of ^{2}H quadrupole-perturbed NMR doublet splitting $\Delta\nu_q$ (a) and of the second moment M_2 (b) for the case of mesogen-labelled (red circles) and crosslinker-labelled LSCEs.

But even more notable are T-dependences of the associated fit parameters σ_θ and α (Fig. 4). Similar behavior in $\sigma_\theta(T)$ is detected for both specimen (Fig. 4a). At low temperatures, in the temperature interval between 300 K and 330 K, σ_θ monotonously increases and is identical in both samples within experimental error. At temperatures around 340 K, a weak anomaly is observed. This could be attributed to the coupling between the smectic and the nematic ordering of the mesogens, which in turn also impacts the orientational order of crosslinker [23,27,28]. The formation of smectic A phase has been detected by X-ray and thermomechanical measurements[23]. At temperatures above 352 K, on approaching the paranematic-nematic transition, σ_θ exhibits a substantial increase. We note that points above 352 K suffer from a large experimental error, both $\sigma_\theta(T)$ and $\alpha(T)$.

Figure 4. Temperature dependences of domain director alignment parameter σ_θ (a) and of motional narrowing effectiveness parameter α (b) for the two selectively labelled components of the LSCE network, the M4 mesogen (red circles) and the V1 crosslinker (green circles).

The motional narrowing effectiveness parameter α increases monotonously with increasing temperature for both mesogen and crosslinker (Fig. 4b), demonstrating that reorientational correlation time τ_Q decreases with temperature ($\tau_Q = \tau_{\mathrm{exch}} \propto \alpha^{-1}$, Eq. (1)). However, in contrast to $\sigma_\theta(T)$, $\alpha(T)$ is detected to be substantially lower for the crosslinker as compared with the mesogen. We find this indicative of slower crosslinker's reorientational dynamics. This observation is also compatible with the T_2 magnetization relaxation results (see section Director reorientation mechanism and domain misalignment) and thus in further support of the scenario where director reorientations of crosslinker molecules are more obstructed, since these are attached to the polymer backbone at both ends, compared with the single side only attachment of mesogen molecules. Temperature dependence of α for mesogen labelling is reminiscent of a motional narrowing transition on increasing temperature, i.e., by the conversion from slow motion regime with $\alpha \ll 1$ at room temperature to fast motion regime with $\alpha > 1$ on approaching paranematic phase at high temperature. With crosslinker labelling, on the other hand, $\alpha \ll 1$ in the whole investigated temperature range, suggestive of slow motion regime due to slow director reorientations. The strong impact of this dynamics on the shape of ^{2}H NMR spectral lines is verified by Fig. 5. Only the crosslinker spectrum (Fig. 5a) resembles inhomogeneously broadened, powder-like shape expected for a relatively large ($\sigma_\theta \approx 20°$) domain disorder. The mesogen spectrum (Fig. 5b) seemingly reflects a state with smaller nematic order S and vanishing domain disorder σ_θ. However, by taking into account almost negligible motional narrowing ($\alpha \approx 0.25$) in the case of crosslinker and a substantial one ($\alpha \approx 3$) in the case of mesogen, both spectra can be modeled with identical S and σ_θ. The difference in α implies difference in reorientational exchange time τ_Q by one order of magnitude ($\alpha \propto \tau_Q^{-1}$).

Figure 5: ^{2}H quadrupole-perturbed NMR spectra of crosslinker-labelled (a) and mesogen-labelled (b) LSCE. Experimental spectra (light green and red lines, respectively) were recorded at $T = 352$ K. Theoretical line shapes (dark green and red lines) were calculated using identical $S = 0.25$ and $\sigma_\theta = 21°$ but different motional narrowing effectiveness parameters α for crosslinker and mesogen, respectively.

Conclusions

Differences in the temperature behavior of local molecular orientational ordering of structurally equivalent LSCEs, with almost identical composition but different deuteration site, either at the mesogen or at the crosslinker, have been studied via ^{2}H quadrupole-perturbed NMR. Contrary to expectations, large differences are detected in the temperature dependence of spectra of the two labelling sites. The observed behavior is attributed to the influence of nematic director's orientational disorder and of its reorientational dynamics. The impact of these processes can be described in terms of a simple model of director reorientational exchange, quantified by only two parameters: the static orientational disorder parameter σ_θ and the motional narrowing effectiveness parameter α. Comparative analysis of theoretically modelled and experimentally determined spectra reveals that crosslinker and mesogen molecules exhibit similar and considerable static orientational disorder ($\sigma_\theta \approx 15°$ at 320 K), which moderately increases with increasing temperature. Contrary to σ_θ, large differences in α are found. This indicates that crosslinker molecules are probed, at all investigated temperatures, in the slow motion regime where the spectrum is inhomogeneously broadened and reflects static disorder in director orientations, whereas mesogen molecules are probed in the slow to fast motion regime with increasing temperature. It is therefore the difference in timescale of director reorientational dynamics, not the difference in the static director disorder, that is responsible for dissimilarities between crosslinker and mesogen spectra.

References

1 M. Warner and E. M. Terentjev, *Liquid Crystal Elastomers*, International Series of Monographs on Physics 120, 2003.
2 W. H. de Jeu, Ed., *Liquid Crystal Elastomers: Materials and Applications*, Springer Berlin Heidelberg, Berlin, Heidelberg, 2012, vol. 250.
3 E. M. Terentjev, *J. Phys. Condens. Matter*, 1999, **11**, R239.
4 V. Domenici, *Prog. Nucl. Magn. Reson. Spectrosc.*, 2012, **63**, 1–32.
5 J. Küpfer and H. Finkelmann, *Makromol. Chem. Rapid Commun.*, 1991, **12**, 717–726.
6 K. A. Burke and P. T. Mather, *J. Mater. Chem.*, 2010, **20**, 3449–3457.
7 V. Domenici, G. Ambrožič, M. Čopič, A. Lebar, I. Drevenšek-Olenik, P. Umek, B. Zalar, B. Zupančič and M. Žigon, *Polymer*, 2009, **50**, 4837–4844.
8 H. Jiang, C. Li and X. Huang, *Nanoscale*, 2013, **5**, 5225–5240.
9 M.-H. Li and P. Keller, *Philos. Trans. R. Soc. Math. Phys. Eng. Sci.*, 2006, **364**, 2763–2777.
10 M. Camacho-Lopez, H. Finkelmann, P. Palffy-Muhoray and M. Shelley, *Nat. Mater.*, 2004, **3**, 307–310.
11 F. Greco, V. Domenici, S. Romiti, T. Assaf, B. Zupančič, J. Milavec, B. Zalar, B. Mazzolai and V. Mattoli, *Mol. Cryst. Liq. Cryst.*, 2013, **572**, 40–49.
12 G. Abbandonato, D. Catalano, V. Domenici and B. Zalar, *Liq. Cryst.*, 2012, **39**, 165–174.
13 V. Domenici and B. Zalar, *Phase Transit.*, 2010, **83**, 1014–1025.
14 V. Domenici, J. Milavec, B. Zupančič, A. Bubnov, V. Hamplova and B. Zalar, *Magn. Reson. Chem.*, 2014, **52**, 649–655.
15 G. Feio, J. L. Figueirinhas, A. R. Tajbakhsh and E. M. Terentjev, *J. Chem. Phys.*, 2009, **131**, 074903.
16 P. J. Sebastião, D. Sousa, A. C. Ribeiro, M. Vilfan, G. Lahajnar, J. Seliger and S. Žumer, *Phys. Rev. E*, 2005, **72**, 061702.
17 A. Abragam, *The principles of nuclear magnetism.*, Clarendon Press, Oxford, 1961.
18 B. Zalar, R. Blinc, S. Zumer, T. Jin and D. Finotello, *Phys. Rev. E Stat. Nonlin. Soft Matter Phys.*, 2002, **65**, 041703.
19 A. Lebar and B. Zalar, *NMR investigation of monodomain liquid crystal elastomer: doctoral thesis*, Ljubljana, 2006.
20 B. Cowan, *Nuclear Magnetic Resonance and Relaxation*, Cambridge University Press, Cambridge; New York, 2005.
21 V. Domenici, M. Geppi and C. A. Veracini, *Prog. Nucl. Magn. Reson. Spectrosc.*, 2007, **50**, 1–50.
22 Z. Luz and S. Meiboom, *J. Chem. Phys.*, 1963, **39**, 366–370.

23 V. Domenici, J. Milavec, A. Bubnov, D. Pociecha, B. Zupančič, A. Rešetič, V. Hamplová, E. Gorecka and B. Zalar, *RSC Adv.*, 2014, **4**, 44056–44064.
24 Sàchez Ferrer Antoni, *Photo-active liquid crystalline elastomers: doctoral thesis*, Barcelona, 2006.
25 A. Lebar, G. Cordoyiannis, Z. Kutnjak and B. Zalar, in *Liquid Crystal Elastomers: Materials and Applications*, ed. W. H. de Jeu, Springer Berlin Heidelberg, 2012, pp. 147–185.
26 C. P. Slichter, *Principles of Magnetic Resonance*, Springer, Berlin ; New York, 3rd enlarged and updated ed. 1990. Corr. 3rd printing 1996 edition., 1996.
27 D. M. Lambreva, B. I. Ostrovskii, H. Finkelmann and W. H. de Jeu, *Phys. Rev. Lett.*, 2004, **93**, 185702.
28 W. H. de Jeu, B. I. Ostrovskii, D. Kramer and H. Finkelmann, *Phys. Rev. E Stat. Nonlin. Soft Matter Phys.*, 2011, **83**, 041703.

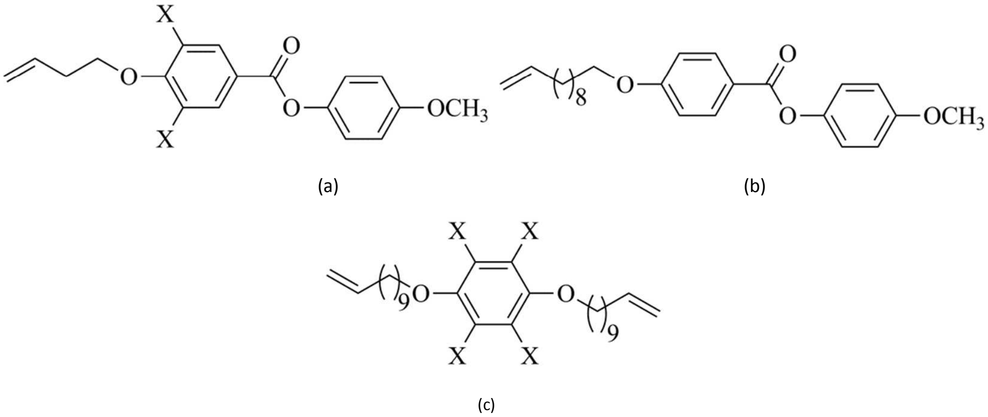

Scheme 1. Chemical constituents of the LSCE film: (a) nematogen M4, (b) smectogen M11, and (c) crosslinker V1. X denotes ^{2}H in selectively labelled compounds.

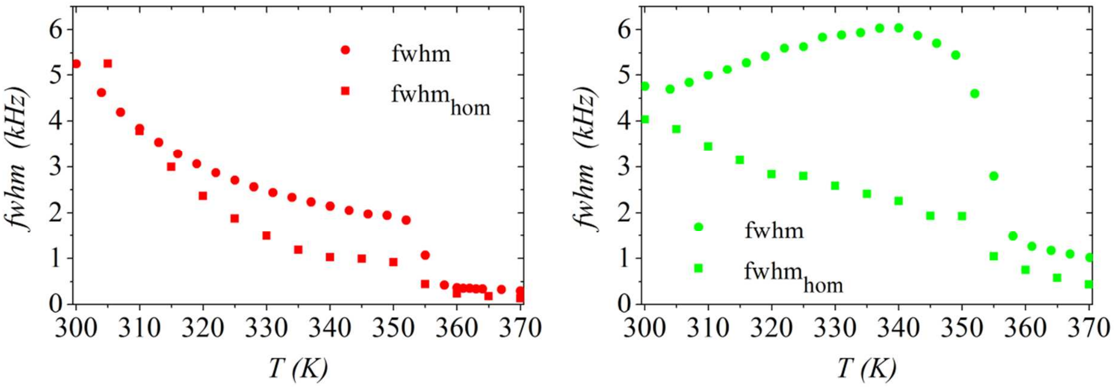

(a)

(b)

Figure 1. Comparison of homogenous line width (as calculated from T_2 measurements) and total linewidth for LSCEs ^{2}H labelled on (a) mesogen and (b) crosslinker.

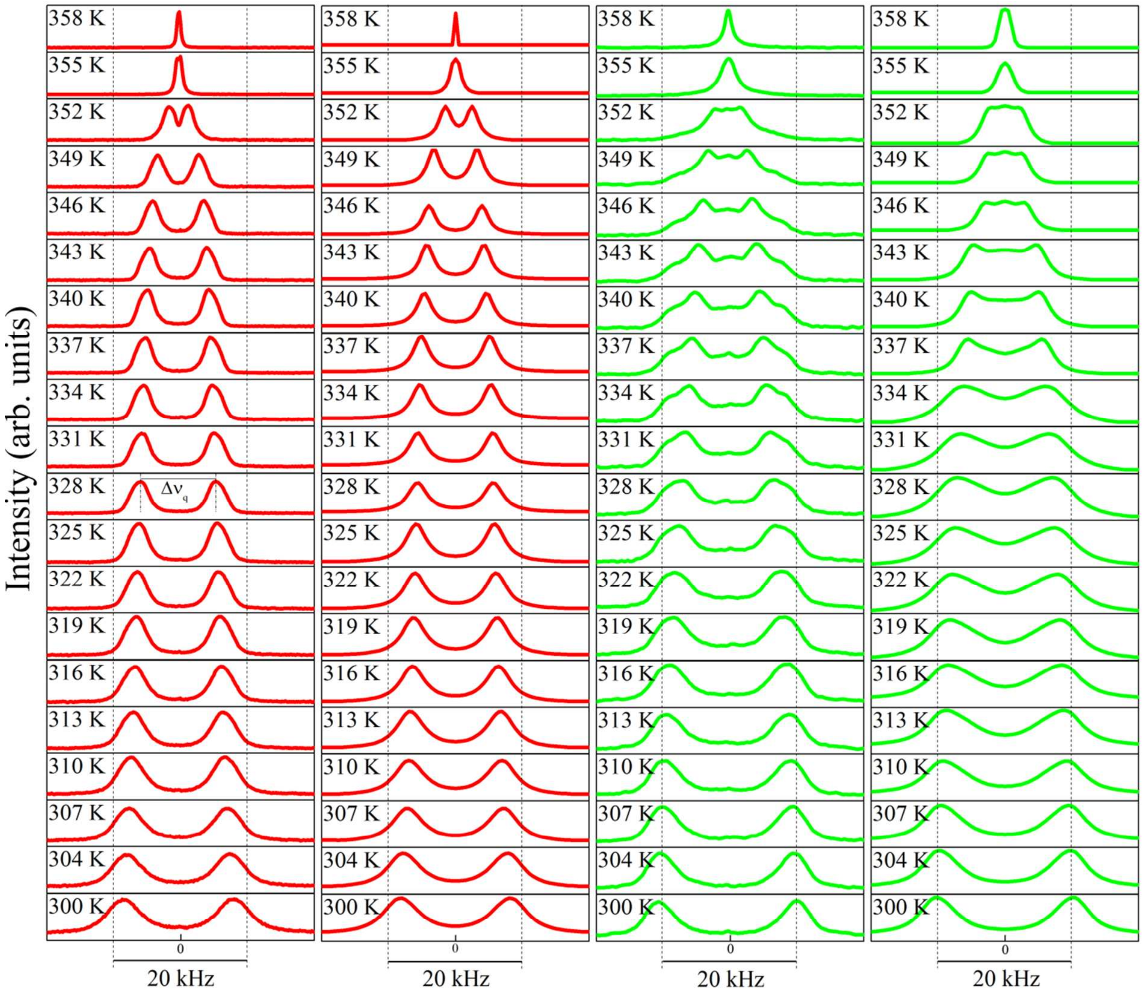

(a) (b) (c) (d)

Figure 2: ^{2}H NMR spectra, recorded from the paranematic to the nematic phase (panel (a) for LSCE labelled on the M4 mesogen and panel (c) for LSCE labelled on the V1 crosslinker) and calculated using the reorientational exchange model of the nematic director (panel (b) for the mesogen and panel (d) for the crosslinker, respectively).

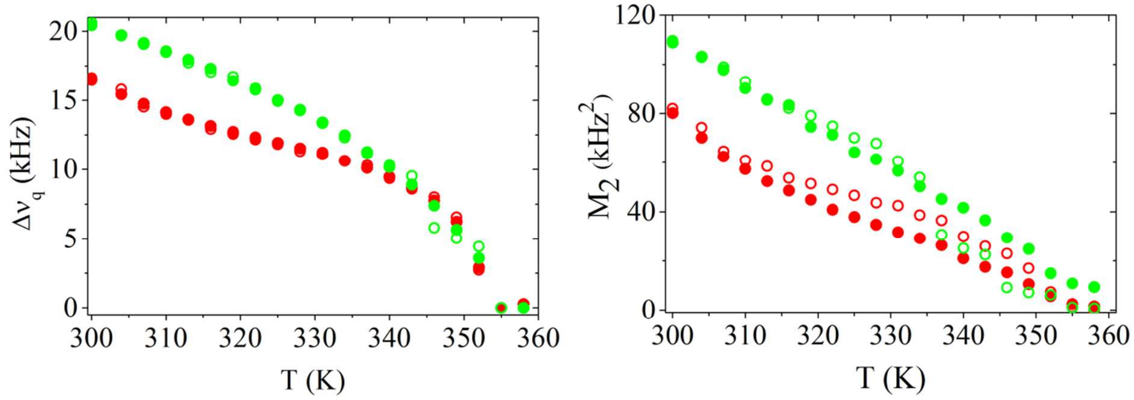

(a) (b)

Figure 3. Comparison of experimental (solid circles) and theoretical (open circles) temperature dependences of ^{2}H quadrupole-perturbed NMR doublet splitting $\Delta\nu_q$ (a) and of the second moment M_2 (b) for the case of mesogen-labelled (red circles) and crosslinker-labelled LSCEs.

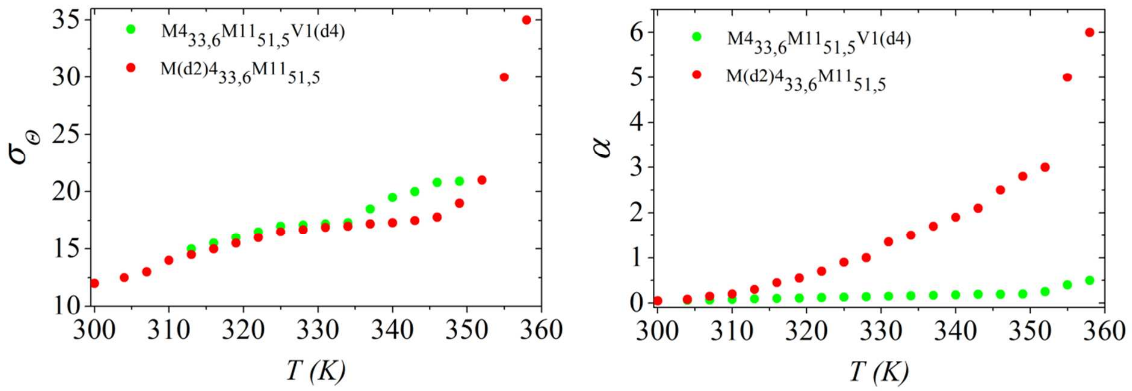

(a) (b)

Figure 4. Temperature dependences of domain director alignment parameter σ_θ (a) and of motional narrowing effectiveness parameter α (b) for the two selectively labelled components of the LSCE network, the M4 mesogen (red circles) and the V1 crosslinker (green circles).

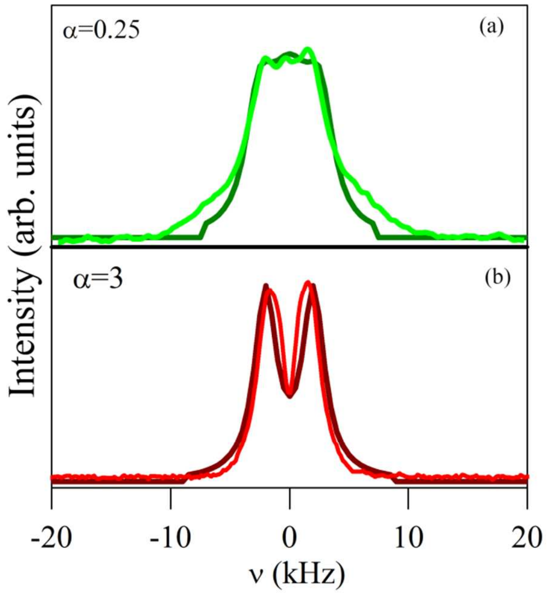

Figure 5: ^{2}H quadrupole-perturbed NMR spectra of crosslinker-labelled (a) and mesogen-labelled (b) LSCE. Experimental spectra (light green and red lines, respectively) were recorded at $T = 352$ K. Theoretical line shapes (dark green and red lines) were calculated using identical $S = 0.25$ and $\sigma_\theta = 21°$ but different motional narrowing effectiveness parameters α for crosslinker and mesogen, respectively.